Journal of Applied Fluid Mechanics, Vol. 13, No. 1, pp. 147-160, 2020.
Available online at www.jafmonline.net, ISSN 1735-3572, EISSN 1735-3645.
DOI: 10.29252/jafm.13.01.30202

Rankine Vortex Formation during Draining: A New Twin Port Suppression Strategy

M. Prabhu[1], R. Ajith Kumar[1†], T. H. Gopikrishnan [1], P. J. Deshpande[2], U. Anandhakrishnan[1], A. S. Kiran[1] and R. P. Govindu[1]

[1] *Department of Mechanical Engineering, Amrita Vishwa Vidyapeetham, Amritapuri, India*
[2] *UAV Division, CSIR-NAL Bengaluru, India*

†*Corresponding Author Email: amritanjali.ajith@gmail.com*

(Received February 25, 2019; accepted June 1, 2019)

ABSTRACT

This paper reveals the results of a study of vortex air core formation (Rankine vortex) when a rotated liquid (water) column in a cylindrical vessel is drained through two ports located at equal eccentricity (e) at the vessel base (diameter, $d_1$and d_2) simultaneously; $d_1$is fixed whereas d_2 is varied. Just before draining, a rotation (n rpm) is provided to the liquid column in controlled conditions. As draining progresses, when the liquid level reaches certain height called critical height (h_c), initially a surface dip forms which further develops in to a vortex extending down till the drain port. Results show that critical height increases as the fluid rotation rate increases at the lowest eccentricity. But, at higher eccentricities, h_c, exhibits more or less an increasing-decreasing trend in most of the cases studied. Critical height is observed to be minimum for the largest value of d_2 (equal to d_1) irrespective of the values of the speed of fluid rotation, liquid initial height and port eccentricity. To particularly note, at the highest eccentricity, vortex formation is found to be completely suppressed for all values of port diameter (d_2) and initial fluid rotation (n) as indicated by the near-zero critical height values. The tangential velocity measurements using Particle Image Velocimetry are also reported. PIV results obtained for certain cases with induced fluid rotation (normal draining and faster draining) correlate well with the changes in the efflux (axial) velocity (deduced analytically) in these cases studied. The tangential velocity along radial direction obtained (PIV) also indicated the type of vortex formed in normal and faster draining cases. Video visualization of vortex formation carried out reveals that, vortex air core switching takes place between the drain ports maintaining an arched or curvilinear surface profile apart from demonstrating the nature of outlet flow discharge. All the vortex air core formation studies so far carried out were invariably with single drain port except the preliminary novel study by the same author group and the present study is a detailed extension of that novel study.

Keywords: Vortexing; Twin drain ports; Liquid draining; Critical height; Time of emptying; PIV; Flow visualization.

NOMENCLATURE

d	diameter of tank	h_{lo}	head loss in no rotation case
d_1	primary port diameter	n	rotational Speed
d_2	secondary port diameter	t_d	time of emptying the tank with rotation
d_{eq}	single equivalent port diameter	t_o	time of emptying the tank without rotation
e	eccentricity		
g	acceleration due to gravity	U_t^*	non dimensional tangential velocity
h_c	critical height	t	arbitrary time instance
h_i	initial height	x	distance measured along radial direction
h_{ld}	head loss in rotation case	ε_d	loss coefficient in rotation case
h_{ls}	head loss due to swirl	ε_o	loss coefficient in no rotation case

1. INTRODUCTION

Vortex air core formation occurs in many thermo-fluid systems such as in liquid propulsion space systems, hydraulic pumping stations, sewage systems, metal casting process and nuclear reactors. When a rotated liquid column contained in a vessel is allowed to drain through an outlet, a vortex-gas core develops as the liquid level reaches certain height, h_c (known as critical height) which subsequently extends down to the outlet partially blocking the outlet area. The immediate consequence of this phenomenon is a reduction of the liquid flow rate from the vessel/tank. In practical applications, this area blockage due to vortex formation is known to cause serious undesirable effects and hence, all the engineering attempts have been to evade it through various means.

Lubin and Springer (1967) have conducted experiments to study the formation of surface dip during liquid draining from a cylindrical tank through a circular concentric port and found that the critical height is independent of the initial height of the liquid column for various liquid-liquid combinations. Furthermore, they derived an expression of the critical height as a function of the discharge flow rate at the drain outlet and liquid density ratio for a given drain outlet diameter. Odgaard (1986) has derived an equation for critical height of vortex air core formation based on a Rankine vortex model and found that h_c is a function of Froude number, Circulation number, Reynolds number and Weber number. Takahashi *et al.* (1988) have experimentally studied the onset conditions for the occurrence of vortex-induced gas entrainment in simple water suction flow into a vertical pipe in a cylindrical tank and have suggested empirical criteria for submergence height based on rotational Froude number and Froude number. Baum and Cook (1975) have experimentally determined the conditions for the initiation of vortex formation with unstable gas core using four different fluids in a cylindrical vessel.

Gluck *et al.* (1966) studied the dependence of gas ingestion height on various non- dimensional parameters. The gas ingestion height was found to be dependent on Froude number, Reynolds number and Bond number at different conditions of draining. The height of the liquid at the tank wall, when gas first reaches the tank outlet, was been determined for a wide range of parameters in their investigation. When the ratio of tank diameter to outlet diameter lied between 20 and 32, the gas ingestion height was independent of the Reynolds number and Bond number and for these conditions, it was found to be depended only on the Froude number.

Literature also cites some interesting works on the suppression of vortexing phenomenon. Abramson *et al.* (1962) found that by employing baffles, vortex formation could be prevented. Drain port geometry could influence vortex formation as reported by Ramamurthi and Tharakan (1992) and in particular, they found that stepped drain port prevents the formation of air core vortex.

Visualization studies using Particle Image Velocimetry with and without suppressor was conducted by Mizuki *et al.* (2003). Water at room temperature was used as the working fluid. They have used a dish type suppressor with suitable mesh size made of brass. Visualization PIV results indicate that their proposed suppressor retards the rotational component of velocity.

In the absence of initial rotation, Gowda *et al.* (1997) proved that vibrations along the horizontal plane can induce vortex formation. This phenomenon was observed only at the natural frequency of free surface oscillation and not at any other frequency. Horizontal vibration suppresses the vortex formation due to rotations in the cases other than at natural frequency. At natural frequency, the vortex is not suppressed. Gowda *et al.* (2013) have methodically studied the effect of cylinder base inclination and reported a limiting value of base inclination beyond which vortex formation is nullified for a particular drain port size value. The suggested reason for vortex suppression is the asymmetry introduced into the flow field due to the base inclination.

Fujimura *et al.* (2004) have reported the vortex break down phenomenon occurring in a cylindrical vessel. Visualization was performed by these authors to capture the salient flow features. In their experiments using a cylindrical vessel with top end wall and, bottom end wall and side wall rotating at different angular velocities, it is revealed that the existence and motion of the vortex break down bubble depends on the ratio between the wall angular velocities. At large value of the angular velocity ratio, bubble ceases to exist.

Mohammadi *et al.* (2012) have studied vortex formation employing bell-mouthed drain-port situated at center of the bottom of the test tank along the cylinder longitudinal axis. Authors proposed introduction of multiple suppressor plates under the bell-mouth drain port to prevent vortex formation. Their studies revealed that critical height and vortex strength can be significantly reduced using this device. In their study, an analytical expression based on Bernoulli equation was formulated and proposed to predict the critical height in a case where vortex suppressor is employed.

As Gowda (1996) reports, vessels with rectangular cross-section (including square) prevent vortexing phenomenon. He argued that the presence of four sharp corners in the square and the rectangular shapes coupled with the non-axisymmetry of the sections prevent the development of rotational motion. In one of the past studies, the same author has shown that a device named dish-type suppressor could eliminate vortex formation (Gowda *et al.*, 1996). Findings of Sohn *et al.* (2008) reveal that drain ports positioned at eccentric locations could control vortex formation.

AjithKumar *et al.* (2016) have revealed that size of the drain outlet port has significant impact on the critical height of the vortex air core formation in a recent study and they suggested that there exists a critical value of drain hole size below which vortexing is annihilated. Quite interestingly,

AjithKumar *et al.* (2017) also found that, at higher eccentricities, higher would be the critical port diameter for vortex suppression. To specifically mention, all these previous investigations were on the application of a single drain port except the preliminary study by the same author group (Gopikrishnan *et al.*, 2017).

As aforementioned, two of the earlier works executed out by Sohn *et al.* (2008) and AjithKumar *et al.* (2016) have reported two feasible strategies for the suppression of vortex air core formation by means of employing suitable drain port size and port eccentricity. But, when the drain port size is reduced below a critical value to suppress vortexing, the immediate consequence would be a diminution in the rate of discharge flow resulting in an increased draining time of the liquid. Quite interestingly, in the case of eccentric ports, port eccentricity itself act as a vortex suppressor (Sohn *et al.*, 2008) and enables a bigger critical port size as revealed by AjithKumar *et al.* (2017). However, it is thought that, when we employ a single eccentric drain port, eccentric location of the port is very likely to induce an overturning couple in space systems such as in liquid propellant tanks (Agarwal *et al.*, 2014). This problem could be eliminated by adopting two eccentric ports for liquid draining from vessels/tanks. As an added advantage, the liquid discharge flow rate from the tank could also be enhanced thereby shortening the time required to empty the tank. It is this aspect which motivated the authors to take up the present study with liquid draining enabled through two drain ports which are eccentrically located at the base of a water filled tank. In the current work, symmetric twin port configuration is studied and is found to provide a solution to this problem.

As already mentioned, all the previous investigations were carried out with only one drain port except the preliminary novel study conducted by the same author group on twin port draining (Gopikrishnan *et al.*, 2017). In the present study, the preliminary study conducted earlier is extended to detail much more features of the vortexing phenomenon and are reported in this paper. The central focus of this investigation is to examine the features of the Rankine vortex phenomenon when a liquid (water) column is drained through two eccentrically located drain ports synchronously which in turn is expected to provide a novel suppression strategy where vortex suppression is achieved without reducing the discharge flow rate.

2. EXPERIMENTAL SETUP DETAILS

As shown in Fig. 1(a), the test cylinder glass tank used for study has an internal diameter (d) of 96 mm and height (h) of 410 mm with its base made out of acrylic plate. At the bottom base of the tank, two drain holes were drilled having different diameters ($d_1$and d_2) as shown in Fig. 1(b) at eccentricity (e); d_1 was fixed at 10 mm whereas d_2 was varied from 4 mm to 10 mm (Fig. 1(b)) to execute a wide range of experiments meeting the objectives of this study. The drain port eccentricities are equal, viz., e as marked in Fig. 1(b); e = 11 mm, 21 mm and 31 mm are employed. Acrylic base plate was glued to the glass cylinder using silicone gel.

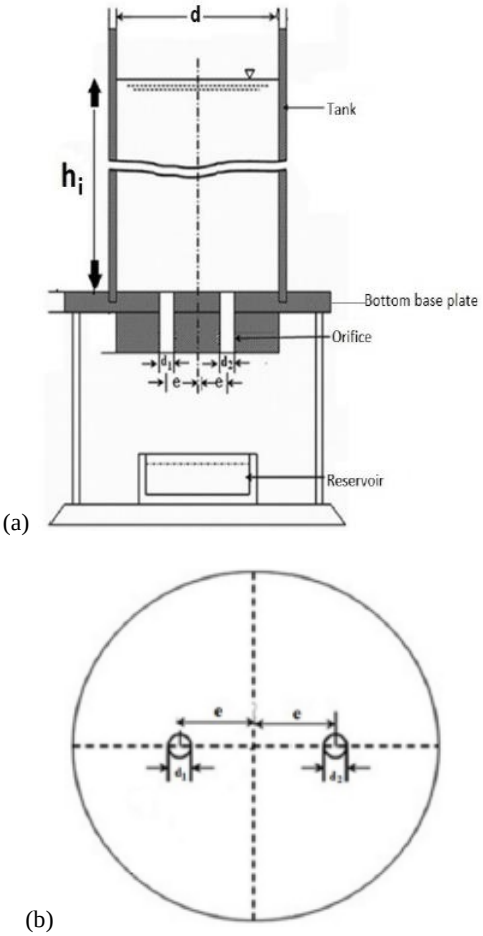

Fig. 1. (a) Test cylindrical tank with two eccentric ports (b) Tank bottom base with two eccentric ports (plan view).

To begin with, liquid (water) was filled in to the tank to an initial height (h_i) and subsequently, a stirrer, which is a straight cylindrical rod made of stainless steel (460 mm long with a diameter of 7.5 mm), was inserted to the bottom of the water level keeping a bottom clearance of 5 mm. The liquid thus filled was induced with a rotation using the stirrer which was driven by an adjustable speed electric motor. Rotation was provided for 2 minutes to impart a uniform angular velocity to the initially still water column. Experiments were conducted for various angular velocities of stirrer in the range 40−200 rpm. After 2 minutes, the stirrer was taken out carefully without affecting the rotation, and the drain port stopper was removed. After the commencement of draining, a surface dip forms which quickly extends down to the drain port forming a vortex with an air core when the liquid level reaches a certain height which was measured as the critical height or critical submergence (h_c) in all the experiments. Liquid height measurement was carried out using a transparent graduated scale vertically attached to the outer cylinder wall. Subsequently, draining was simultaneously enabled through two drain ports with diameters d_1 and d_2 where d_1 was fixed (=10 mm)

as mentioned earlier whereas d_2 was varied assuming values 4 mm, 6 mm, 8 mm and 10 mm. Henceforth, d_1 is referred to as primary port and d_2 is referred to as secondary port. Also, this study was conducted at three values of initial height of the liquid column (h_i), viz., 300 mm, 350 mm and 400 mm. The liquid used was clean water at room temperature ($\sim$28℃). The measured quantities in this study are critical height and time of emptying. To check the repeatability of experiments, each experimental case was repeated 10 times. From such experimental trails, the standard deviation values of critical height and time of emptying were estimated. Correspondingly, the un-certainty in the measurements of these parameters, viz., critical height and time of emptying was estimated to be 11% and 7% respectively.

To have a better understanding of the physics of the vortex flow, 2D Particle Image Velocimetry technique was employed. PIV measurements were performed at UAV Division, CSIR-NAL, Bangalore, INDIA. PIV setup consists of a Litron make 100 mJ and 100 Hz dual cavity Nd-YAG Laser setup, 4 MP Phantom High Speed Camera and the light arm & Laser optics to create a Laser sheet. A horizontal Laser sheet passing through cross-section of the tank at distance of 50 mm from the acrylic base was created and the high speed camera was mounted firmly to the Linous railing on top of the tank as shown in Fig 2. Immediately after the removal of the stirrer, drains ports were opened and 600 image pairs were captured at a sampling rate of 50 Hz while tank was emptying. The time delay between each image pair was adjusted to 100 microseconds. TSI Insight 4G software was used to acquire and process the images. Processing was done with 32 X 32 interrogation window with 50 % overlap with a resolution of 1 mm in 185 X 155 mm field of view along X and Y axes respectively. A time-averaging of the data was done over every 20 image pairs (0.4 second data is averaged).

For some typical cases, video shooting of the draining process was conducted to visualize the vortex-air core formation and the features of the flow discharge at the drain port exit using SONY high denition camera (Make: SONY DSR-PD150) and the video was recorded at 25 frames per second.

3. RESULTS AND DISCUSSION

3.1 Quantitative Analysis

Results are presented in Figs. 3(a) – 8(c) as dimensionless critical submergence ($H_c = h_c/h_i$) and dimensionless time of draining ($T_d = t_d/t_o$) versus non dimensional fluid rotation speed (N = n * 1 minute) plots; t_d is the time required to completely drain out the liquid from the tank with liquid column rotation and t_o the time taken for complete liquid draining without fluid rotation. In these figures avaraged values of critical height and time of draining were utilised. To recapitulate, liquid is drained out through two drain holes simultaneously with non-dimensional diameters D_1 and D_2 ; $D_1 = d_1/d$ is fixed (= 0.10) whereas $D_2 = d_2/d$ is varied and takes values 0.04, 0.06, 0.08 and 0.10. It is pointed out that, liquid emptying time with no rotation (t_o) varies with d_2/d_1 ratio. More details on variation of t_o with respect to d_2/d_1 ratio are furnished towards later in this section. Results are given for various non-dimensional eccentricities, viz., $E = e/d$ (0.11, 0.22 & 0.32). Comparative statements with respect to single drain port results appear in many parts of the text and hence, hereafter, single drain port is abbreviated as SDP.

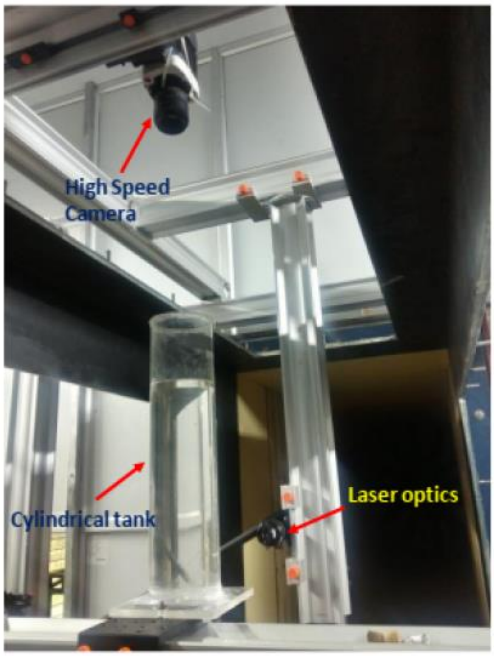

Fig. 2. Experimental Setup for PIV.

Figures 3(a) – 3(c) show the variation of H_c w.r.t N at E = 0.11 for various values of h_i. In Fig. 3(a), the standard deviation values of critical height (non dimensional) is shown for all D_2 values. As could be seen, H_c registers an increasing trend as N is increased irrespective of D_2 value. Higher critical submergence indicates an early vortex formation which also means that vortexing is more intense. As Fig. 3(a) shows, an increase in D_2 brings a reduction in the critical height at a given value of N for all the cases of h_i values tested. That means, the intensity of vortexing diminishes as D_2 increases and this finding is quite contrary to SDP results. For the case of SDP, critical height is greater at larger drain port size (AjithKumar *et al.*, 2016; AjithKumar *et al.*, 2017)

Critical submergence variation with respect to fluid rotation speed is nearly the same at all values of liquid initial heights as seen in Figs. 3(a) – 3(c). But, results indicate that, with fluid rotation rate, there are minor variations in the H_c trends at different h_i values at this eccentricity (E = 0.11).

Figures 4(a) – 4(c) show the dimensionless time needed to vacate the tank in correspondence with the critical submergence depicted in Figs. 3(a) – 3(c) (E = 0.11) at all h_i values. In Fig. 4(a), the standard

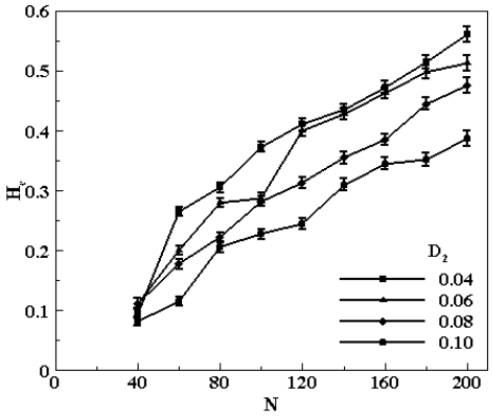

(a) h_i = 400 mm

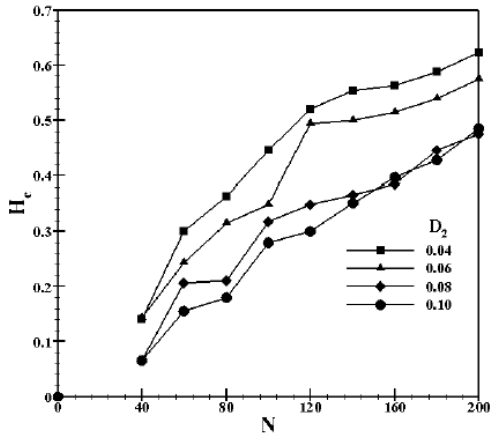

(b) h_i = 350 mm

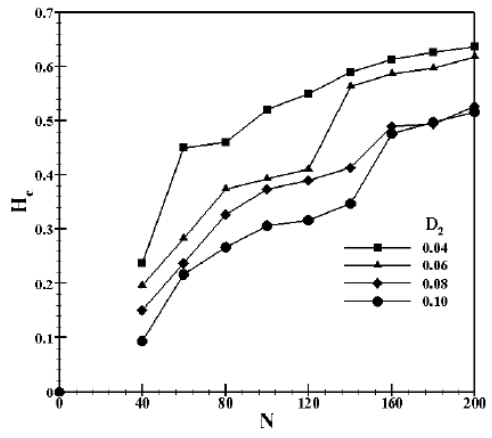

(c) h_i = 300 mm

Fig. 3. Dimensionless critical height versus N at E=0.11.

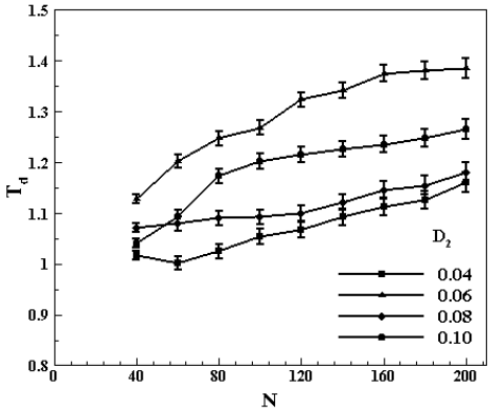

(a) h_i = 400 mm

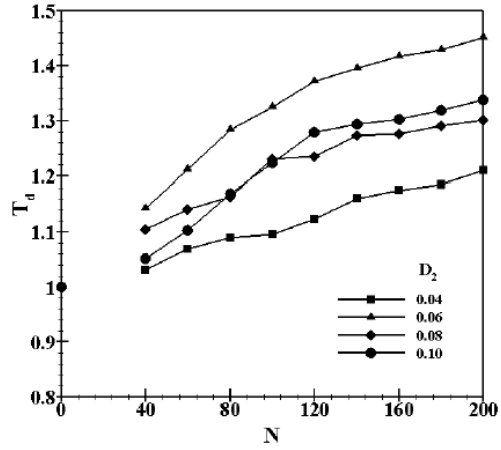

(b) h_i = 350 mm

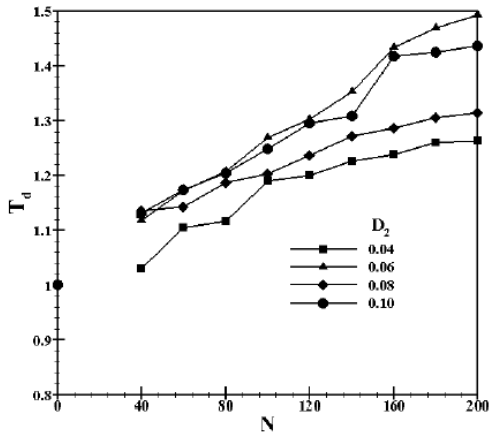

(c) h_i = 300 mm

Fig. 4. Dimensionless time of emptying versus N at E = 0.11.

deviation values of time of draining (non dimensional) is shown for all D_2 values. In general, T_d value rises with N similar to the trend of H_c. Further, as seen in these figures, at all h_i values, T_d is the highest for $D_2 = 0.06$ and is the least for $D_2 = 0.04$. No systematic trend is observed for the variation of time of draining with D_2. Paradoxically, as port size increases, dimensionless emptying time also becomes larger for a SDP irrespective of its location (concentric/eccentric) because critical

submergence increases (AjithKumar *et al.*, 2016; AjithKumar *et al.*, 2017). At higher critical heights, vortex air core forms early and blocks the drain port reducing the discharge flow rate. At reduced flow rate conditions, emptying time with liquid rotation (t_d) becomes longer for an isolated (single) drain outlet.

Moreover, the liquid emptying time with no rotation imparted (t_o) decreases as port size increases for the case of SDP at a given initial liquid column height (h_i) because, in this case, discharge volume flow rate increases with bigger port size, flow rate being directly proportional to the port area. Hence, enhancement of T_d is due to multiple reasons in that case, i.e. increase by virtue of both port diameter as well as higher H_c value. Although, as mentioned earlier, such a regular trend w.r.t drain port size is not seen in the case of twin drain port presumably due to the non-linear variations the liquid emptying time with fluid rotation and without it (t_d & t_o) undergo by virtue of the flow interference between the drain ports during liquid draining process. This sporadic trend in $T_d$with respect to D_2 is seen in all cases as could be observed in Figs. 4(a) – 4(c).

At an increased value of port eccentricity, viz., E = 0.22, considerable changes occur in the critical submergence values as depicted in Figs. 5(a) – 5(c) irrespective of the value of initial liquid height. Barring the case with $D_2 = 0.04$, H_c at first increases followed by a decreasing trend with N culminating in substantially smaller values at N = 200. For $D_2 = 0.04$, H_c exhibits a sharp increase at first at around N = 40 − 60 and then, gradually escalates for N > 80 ending up in smaller but notable values of $H_c(\sim 0.4)$. That is, except for $D_2 = 0.04$, vortexing is suppressed for $D_2 = 0.06$, 0.08 and 0.10 at the highest speed tested (200 rpm). This again is quite antithetical to the expectations because, as mentioned before, for SDP, at larger port diameters, critical submergence will be more which indicates a more acute vortexing phenomenon. It appears that, in twin port draining, one drain port acts as a vortex suppressor to the other. Critical height reaches the peak in the rotational speed range 100 rpm < n < 150 rpm at all h_i and D_2 values. To specifically highlight, $D_2 = 0.10$ represents the case of identical twin ports (equal diameters) in which case the vortex formation is significantly suppressed in the entire speed range excluding n = 120 rpm. The highest critical submergence value observed in the all these cases (E = 0.22) is notably lower than that for E = 0.11. Figures 6(a) – 6(c) show the corresponding dimensionless liquid emptying time (T_d) where, a gradually rising characteristic could be seen at all values of h_i. To specifically note, in the speed range 40 rpm < n < 120 rpm, T_d goes below 1.0 for $D_2 = 0.04$ for $h_i = 400$ mm and 350 mm indicating a faster liquid draining process for the case with rotation compared to the case of no fluid rotation.

At still higher port eccentricity (E = 0.32), the course of the critical submergence changes as shown in Figs. 7(a) – 7(c). As N increases, H_c increases, attains the peak value after which it diminishes in general. At $h_i = 400$ mm, the case with $D_2 = 0.04$ registers the highest critical submergence, viz., $H_c \sim 0.12$ ((Fig. 7a) which is significantly lesser than the maximum critical height values at the smaller eccentricity values (= 11mm, 21mm); peak (highest) H_c value attenuates by about 78% in comparison with the case at e = 11mm (E = 0.11). For higher D_2 values, vortexing is very weak as reflected in the substantially reduced H_c values at this h_i value. At lower h_i values (= 350 mm and 300 mm), vortexing intensity greatly drops as reflected in the significantly lower H_c values of the order of 10^{-2} for $D_2 = 0.08$ and 0.10 (Figs. 7b & 7c). That means, extremely feeble vortex air core forms during the last stages of liquid draining at this value of eccentricity. *To highlight, vortex formation is totally suppressed for D_2=0.10 (case of identical twin drain ports) irrespective of the value of the initial liquid level*. The corresponding trends of time of emptying are shown in Figs. 8(a) – 8(c) where the overall trends could be seen to be noticeably different from the graphical trends of emptying time at lower eccentricities previously dealt with. However, like for lower eccentricities, in this case also, there is no organized trend for the variation of T_d with respect to N at all values of initial liquid level (h_i). A common feature observed is that, for $D_2 = 0.06$, for N > 120, T_d drops down reaching substantially lower values (T_d< 1.0) for all h_i values. For $D_2 = 0.08$, around N = 140, T_d < 1.0 for $h_i = 350$ mm and 400 mm. Both these traits imply that process of draining becomes quicker when rotation is imparted to the fluid.

The main thrust of this paper is to reveal the advantage of employing two eccentric drain ports instead of one in the matter of suppressing air core vortex formation. As already mentioned earlier, even without any fluid rotation imparted (plane draining case), the time of draining varies for different $d_1 - d_2$ port combinations. In this context, it is necessary to know the change in t_o with d_2/d_1 ratio (= D) which is typically shown in Fig. 9 for all eccentricity values considered in this study, viz., E = 0.11, 0.22 and 0.32. As Fig. 9 shows, t_o reduces as D increases (as expected) but in a non-linear fashion characterized by a steep decrease followed by a relatively gradual reduction irrespective of the value of E. It could also be seen that, beyond D = 0.8, t_o remains nearly constant for higher values of E (= 0.22, 0.32). A concept of equivalent port is introduced here to facilitate the comparison between draining (plane draining) through twin ports with that through a single equivalent port located at the eccentric primary port position. A single equivalent port (diameter, d_{eq}) is defined as the one which carries an area equal to the sum of the areas of primary and second ports in no rotation case (plane draining) such that discharge flow rate remains the same for both (twin ports and equivalent drain port) in ideal conditions. Variation of t_o with respect to D for various eccentricities at $h_i = 400$ mm is given in Fig. 9. In this plot, t_o values for various values of D_{eq} (= d_{eq}/d) at E = 0.11 are also incorporated. As an interesting note, for the lowest D value, time of

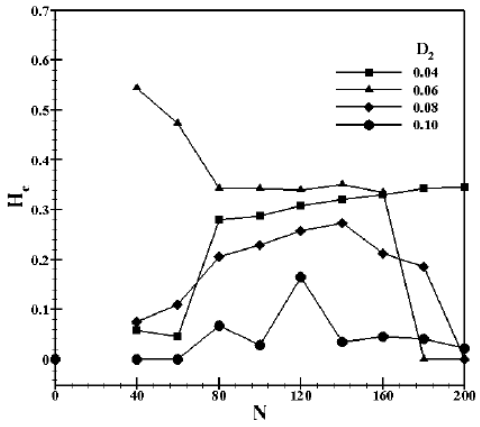

(a) h_i = 400 mm

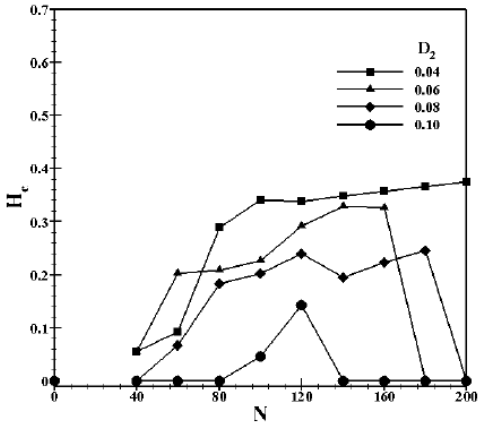

(b) h_i = 350 mm

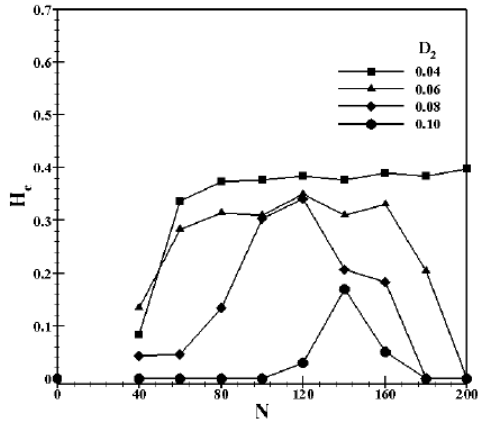

(c) h_i = 300 mm

Fig. 5. Dimensionless critical height versus N at E = 0.22.

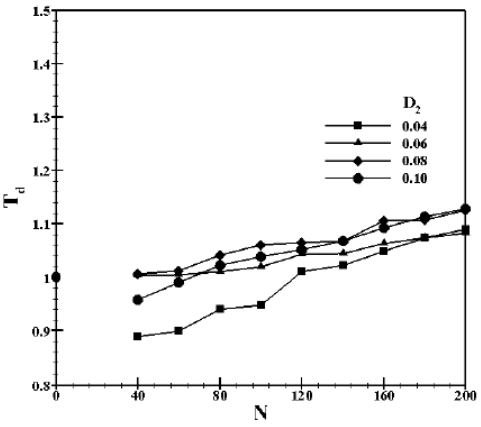

(a) h_i = 400 mm

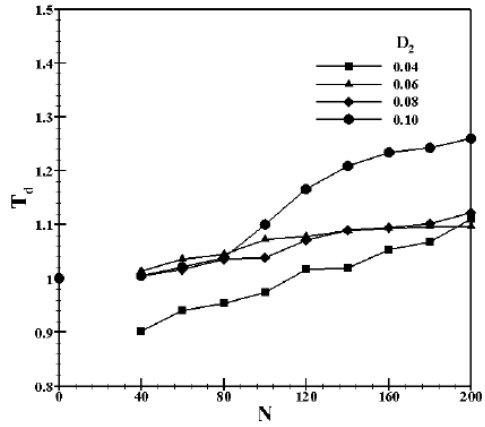

(b) h_i = 350 mm

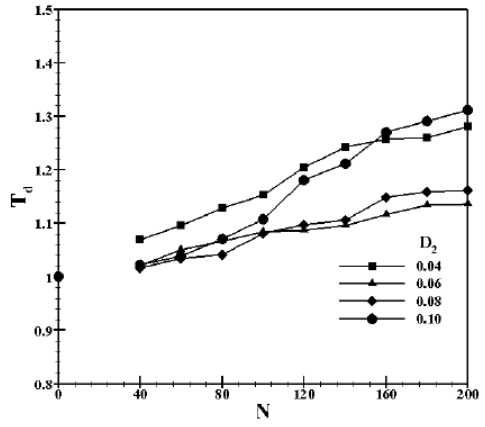

(c) h_i = 300 mm

Fig. 6. Dimensionless time of emptying versus N at E = 0.22.

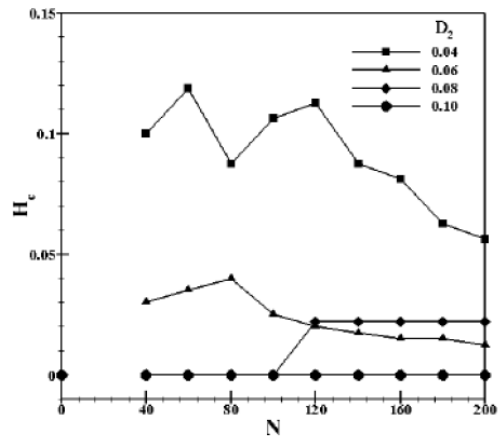

(a) h_i = 400 mm

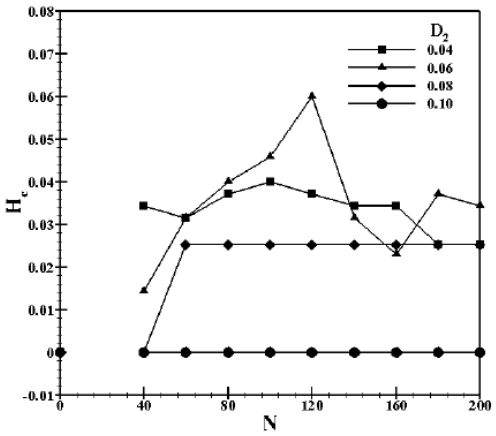

(b) h_i = 350 mm

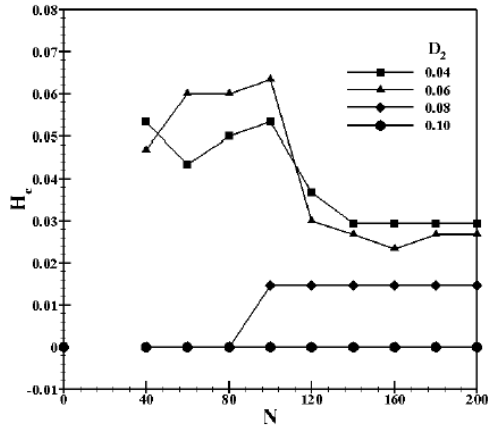

(c) h_i = 300 mm

Fig. 7. Dimensionless critical height versus N at E = 0.32.

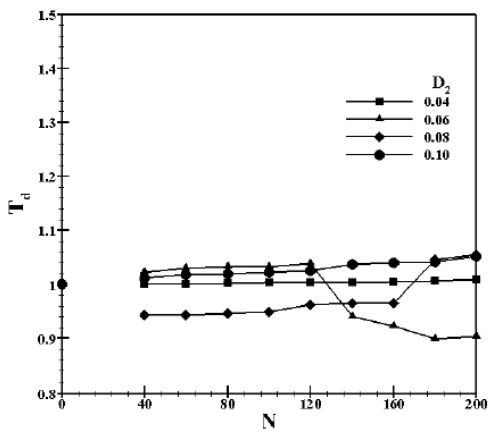

(a) h_i = 400 mm

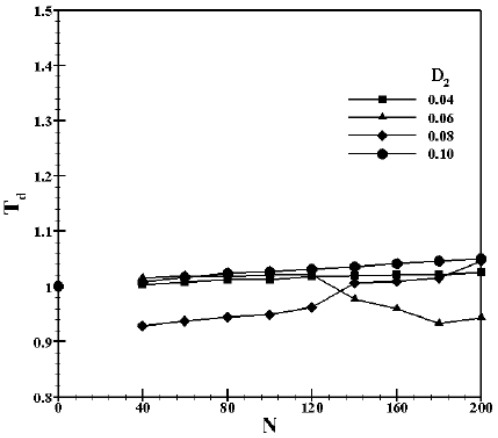

(b) h_i = 350 mm

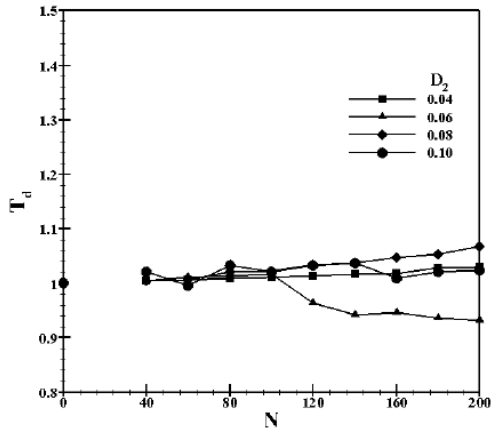

(c) h_i = 300 mm

Fig. 8. Dimensionless time of emptying versus N at E = 0.32.

draining for twin port configuration is notably different from that of the equivalent port by about 28% (of the time draining of the equivalent drain port) but at higher D values, the difference between them substantially reduces as Fig. 9 shows. This result indicates that, there could be some flow interference effects between the drain ports even in the absence of fluid rotation.

For a specific $d_1 - d_2$ combination, variation of

$t_o$with eccentricity varies within 16% to 20%. The trend is similar for other initial heights (but not presented here).

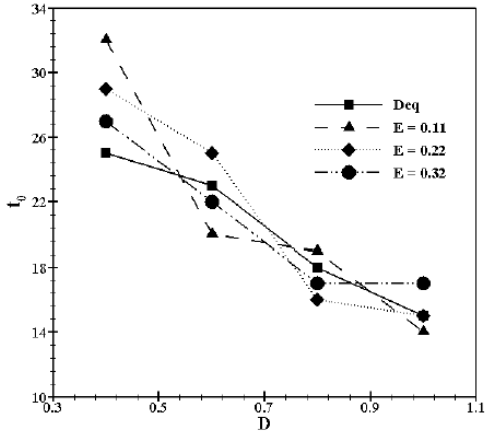

Fig. 9. Variation of t_o with D for various eccentricities.

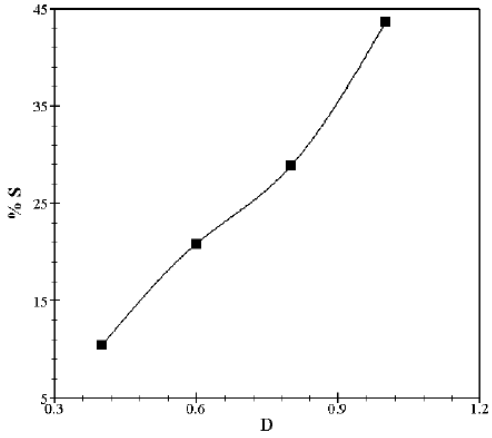

Fig. 10. Variation in Percentage of suppression with D.

Experiments were conducted with single equivalent port for all D values to assess the effectiveness of twin drain port draining. It was observed that compared to single port draining, twin ports can suppress air core vortex more efficiently for all configurations studied as shown in Fig. 10. In Fig. 10, S is defined as the ratio of difference in critical height obtained with twin port and the corresponding single equivalent port to the critical height of equivalent drain port at $h_i = 400$, n = 200 rpm and E = 0.11; E = 0.11 is chosen because it is at this E value the maximum critical height is obtained. Figure 10 reveals that highest suppression (S) of 43.6% is obtained at D = 1.0 which is a significant value from practical point of view and as D reduces, suppression of vortexing reduces. *This result clearly suggests that, for liquid draining, employing two drain ports could certainly be preferred over a single equivalent port for efficient suppression of vortexing phenomenon at identical conditions*.

Figure 11 shows the video snap shots of the initiation and subsequent development of the vortex air core (soon after the commencement of liquid draining) from the instant of formation of surface dip at the 6^{th} sec and subsequent critical submergence of vortex in the very next instant (7^{th} sec) at E = 0.11, $D_2 = 0.04$, $h_i = 350$ mm & n = 200 rpm. In these photographic images, long white line indicates the cylinder center line and short line show the center line of the drain port. These lines are marked to understand the motion of the vortex air core and its sway to either sides clearly. As draining progresses, vortex air core swings about the vertical vessel axis to touch the eccentrically located drain holes as seen in Fig. 11. As seen here, in the 19^{th} sec, vortex air core shrinks to form a dip, then extends again to form the full vortex (t = 19.5 sec) and subsequently, it once again assumes a kink shape (t = 19.9 sec) soon after which it develops in to a full vortex (t = 20 sec). This switching of air core possibly indicates alterations in the flow structures in the near vicinity of the drain outlets.

The switching of vortex air core could be explained as follows. At the beginning of fluid rotation (drain port in the closed condition) the vortex axis will be aligned along the cylinder axis. But, when the liquid draining starts, vortex axis shifts towards the eccentric port axis. According to Piva *et al.* (2003), at this point of migration of vortex axis towards the eccentric port axis, vorticity is greatly amplified due to gradient of axial flow (vertical direction) and the free surface is drawn down. After migration of vortex axis towards one of the drain ports, as could be seen from Fig. 11, vortex air core withdraws back to its dip configuration (become a small dip) before it switches to the other drain port. This could be possibly due to changes in flow condition around the drain port while draining takes place. Authors consider that this is a kind of nonlinear phenomenon associated with vortexing for which exact reasons are not known at present. Authors believe that further studies are required to bring to light the flow physics behind the switching phenomenon of vortex air core. From the recorded video analysis, the average switching frequency is found to be 1.3 Hz

For E = 0.32, a generic feature noticed is that, for $D_2 = 0.06$, N > 120, H_c drops down reaching lower values (see Figs.7a – 7c) together with shorter draining time (see Figs. 8a – 8c). As mentioned earlier, for $D_2 = 0.08$, up to N = 140, T_d value goes below unity at $h_i = 350$ mm and 400 mm which implies that quicker draining happens when the liquid column is induced with rotation plausibly suggesting a different mechanics of flow in the drain port vicinity. Video snapshots presented in Fig. 12 reflect this faster draining process as described below.

Figure 12 shows the flow discharge features in a case where no vortex formation occurs ($h_c = 0$). As seen in this figure, at the instance when the drain ports are opened, i.e. time t = 0 s, the water jet from the primary drain port appears wider (thicker) and turbulent compared to the jet discharge from the secondary drain port. At t = 1 s, the jet from primary

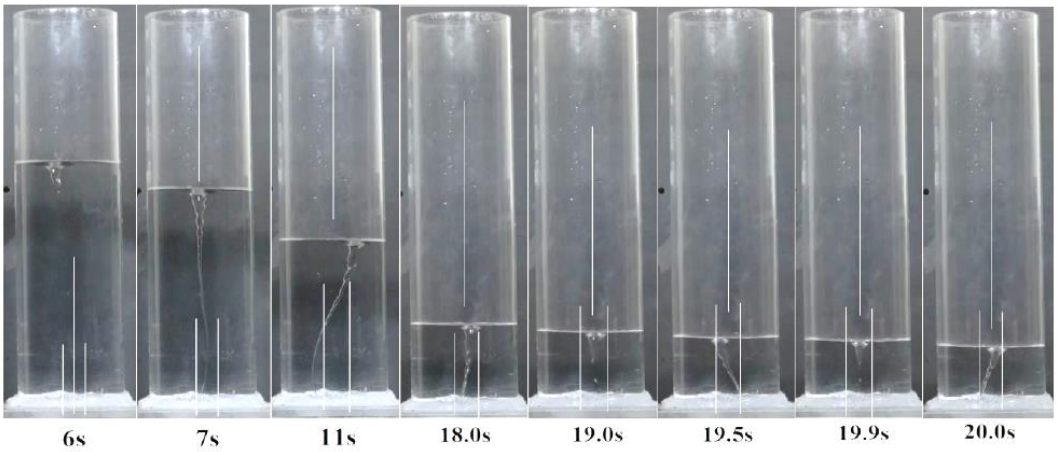

Fig. 11. Vortex air core switching between drain ports at E =0.11, D_2=0.04, h_i=350 mm & n=200 rpm.

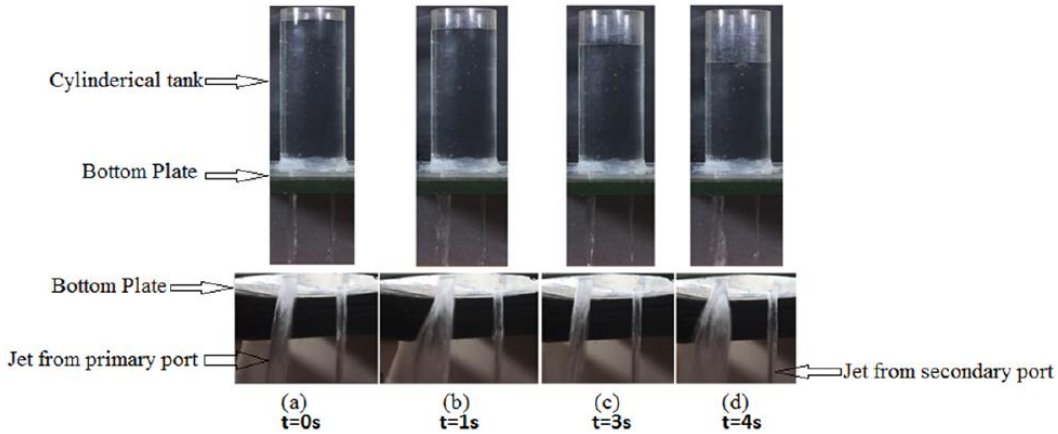

Fig. 12. Drain port exit flow features in a fast draining case: D_1 = 0.10, D_2 = 0.06, E = 0.32, h_i = 350 mm and n=200 rpm.

drain port spreads out more like a sheet and subsequently at t = 3 s, it assumes back its near-cylindrical shape. Further at t = 4 s, the discharge jet becomes more wide again. Throughout the draining, small surface dip (kink) kept appearing and disappearing at some time instances which never developed in to a vortex air core. The water jet from the secondary port has a quite smooth cylindrical shape throughout the draining with diameter roughly equal to the drain port diameter. To quantify these discharge observations, water discharge from both the drain ports were collected in a graduated beaker and measured separately for rotation and no rotation cases. It was found that, with rotation, mass of water collected from the primary and secondary ports were 30% and 2% greater respectively compared to the corresponding no rotation cases. This observation corroborates well with the analytical deductions and the PIV results discussed in next section.

3.2 Tangential Velocity Distributions measured by Particle Image Velocimetry

The PIV results presented in Figs. 13 and 14 represent the velocity contours superimposed with stream lines and tangential velocity distribution along radial direction (X-axis, 'x' being measured from one wall to other connecting the cylinder centre) at time instant t = 4.2 sec after opening of drain ports. The results are shown for the two cases; one being faster draining (E = 0.32, D_1 =0.1 & D_2 =0.06) and the other being the normal draining (E = 0.11, D_1 =0.1 & D_2 =0.08) for n = 200 rpm and h_i = 350 mm. For the same imposed rotational velocity (n = 200 rpm), it can be seen from Fig. 13(a) (faster draining case) that, fluid tangential kinetic energy is notably lower than that for the normal draining case (Fig. 14(a)). In figures (Figs. 13(b) and 14(b)), tangential velocity distribution along radial direction is presented to distinguish the nature of vortex formation in these cases. In Fig. 13(b), (fast draining case), the eccentric drain port location (primary port) is at E = 0.32, that is at x/d = 0.82. From this figure it could be seen that, at about x/d = 0.8, the tangential velocity distribution is characterised by a dip (at x/d~ 0.8) with increase in velocity values towards either sides reaching peak values at about x/d = 0.67 and x/d = 0.85. For x/d < 0.67 and x/d > 0.85, the velocity value reduces. This implies a tendency to form a weak Rankine vortex. A video analysis carried out for this

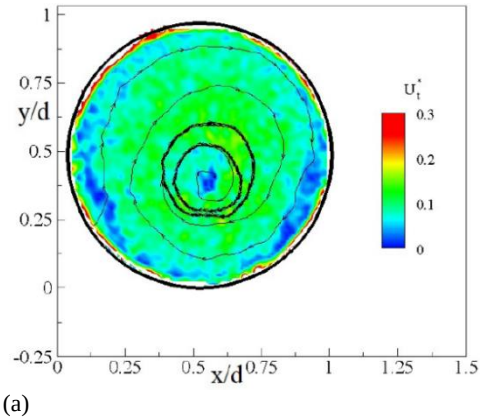

(a)

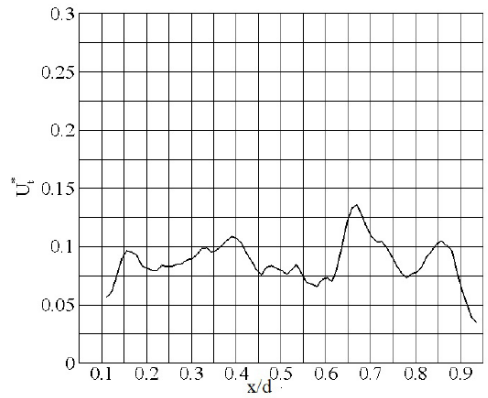

(b)

Fig. 13. PIV Image showing velocity contour & tangential velocity along radial direction: E=0.32, $D_1 = 0.10$ & $D_2 = 0.06$.

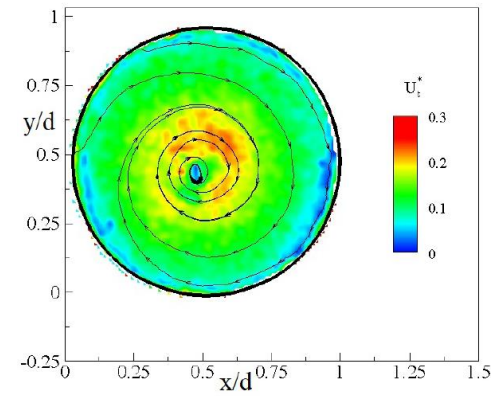

(a)

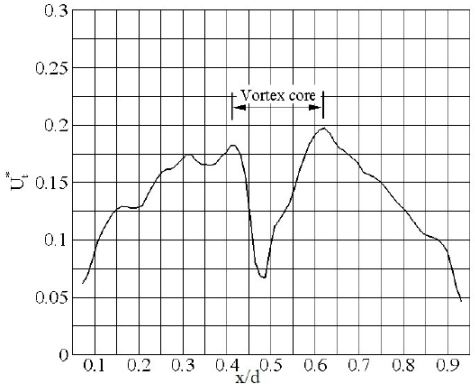

(b)

Fig. 14. PIV Image showing velocity contour & tangential velocity along radial direction: E = 0.11, $D_1 = 0.10$ & $D_2 = 0.08$.

case have also shown that subsequent to draining, there is a deep dip formation aligned with the primary port axis. But, this is not extending down to become a full Rankine vortex. Video snapshot for this case is not presented here due to space constrains. Whereas in Fig. 14(b) at $x/d \sim 0.45$, a sharp dip is seen from which velocity steeply increases towards either sides reaching the peak values at about $x/d = 0.42$ and $x/d = 0.65$ characterising a forced vortex with core diameter 0.2d. For $x/d < 0.42$ and $x/d > 0.65$ velocity decreases as seen in the figure which characterises a free vortex flow. Thus, this velocity distribution clearly shows a Rankine vortex formation in this case which is also reflected in velocity contours (Fig. 14a). Rankine vortex (Odgaard, 1986) which formed in this case blocks the drain port outlet reducing the discharge flow rate thus increasing the time of draining (see Fig. 4b).

3.3 A Mathematical Treatment to the Observed Features

The (efflux) velocity of the liquid at the drain port just at the beginning of draining could be expressed as follows

$$V_0 = \sqrt{2g\,(h_i - h_{lo})} = \varepsilon_0 \sqrt{2gh_i} \tag{1}$$

$$V_d = \sqrt{2g\,(h_i - h_{ld})} = \varepsilon_d \sqrt{2gh_i} \tag{2}$$

where h_l indicates the head loss and ε is the loss coefficient defined here with subscripts o & d indicating no rotation and rotation cases of liquid respectively. The head loss during the draining process varies with the liquid height which includes (a) the head loss at entry and exit of the drain port (b) the head loss due to friction in the drain port (c) other hydraulic losses possibly occurring during draining in swirling flows. The coefficients ε_o and ε_d takes care of the head losses (a), (b) and (c) mentioned above. To specifically mention, just at the start of draining, loss is limited to (a) and (b) only. As time progresses, other hydraulic losses comes in to picture which possibly varies during draining.

From Eqs. (1) & (2), we can write as

$$\varepsilon_0 = \sqrt{1 - \frac{h_{lo}}{h_i}} \tag{3}$$

$$\varepsilon_d = \sqrt{1 - \frac{h_{ld}}{h_i}} \tag{4}$$

It could be shown from fundamentals that the drain time of the liquid column without and with fluid rotation are

$$t_o = \frac{1}{\varepsilon_0}\left(\sqrt{\frac{2h_i}{g}}\right)\left(\frac{d^2}{d_1^2+d_2^2}\right) \quad (5)$$

$$t_d = \frac{1}{\varepsilon_d}\left(\sqrt{\frac{2h_i}{g}}\right)\left(\frac{d^2}{d_1^2+d_2^2}\right) \quad (6)$$

Where d_1 , d_2 are port diameters in twin port configuration.

As previously mentioned, coefficients ε_o and ε_d vary with respect to time (during draining). This aspect was checked with known values of critical height and the corresponding time of draining (Figs. 3−8). Therefore, the values assigned to these loss coefficients are the time averaged values in Eqs. (5) and (6).

For normal draining, from the results (typically see Fig. 4), it can be seen that

$$t_o < t_d \quad (7)$$

t_o is less than t_d because the drain port area is obstructed by the tip of the Rankine vortex during its genesis as mentioned earlier. Correspondingly, from Eqs. (5), (6); it could be deduced that

$$\varepsilon_0 > \varepsilon_d \quad (8)$$

Subsequently, Eqs. (3), (4) would show that

$$h_{lo} < h_{ld} \quad (9)$$

where h_{lo} is the head loss in case where no fluid rotation is imparted and h_{ld} is the head loss in case of fluid rotation which includes the additional head loss due to fluid swirling (h_{ls}).

$$h_{ld} = h_{lo} + h_{ls} \quad (10)$$

To highlight, the parameters h_{lo} and h_{ld} in Eq. (9) are arrived at considering the time averaged values of the coefficients ε_o and ε_d over the total draining time (time of emptying). Comparing Eqs. (9) & (10), it can be inferred that h_{ls} is positive. From Eq. (2), the efflux velocity of liquid draining can be re-written as

$$V_d = \sqrt{2g(h_i - h_{ld})} = \sqrt{2g(h_i - (h_{lo} + h_{ls})} \quad (11)$$

For fast draining, it is obvious that

$$T_d < 1.0 \Rightarrow t_0 > t_d \quad (12)$$

Correspondingly, from Eqs. (5) & (6), it could be deduced that

$$\varepsilon_0 < \varepsilon_d \quad (13)$$

Equations (3) & (4) gives

$$h_{lo} > h_{ld} \quad (14)$$

Substituting Eq. (14) in Eq. (10), it can be inferred that h_{ls} is negative.

For normal draining case, h_{ls} is positive which means that efflux velocity would reduce due to this loss (associated with swirl flow) following Eq. (11).

When h_{ls} is negative, we obtain that the efflux velocity would correspondingly increase which is obviously a fast draining case. That is, the kinetic energy associated with the axial flow (which assist in draining) increases. In the context of equal initial rotational kinetic energy provided to the liquid column (at n = 200 rpm) to both the cases (normal and fast draining), this increase in efflux velocity indicates a possible reduction in the rotational kinetic energy associated with the swirl flow in the case of fast draining. In other words, negative h_{ls} points to the possibility of a reduction in the tangential velocities which genuinely complies with the PIV results (Fig. 13a). Quite interestingly, this aspect of increase in efflux velocity could be seen reflected in the flow visualization results also (Fig. 12) where the discharge flow exit from the primary port appears much wider (like a sheet) and turbulent with higher discharge flow rate (30% higher than no rotation case) as discussed before.

The present study has significant practical relevance in the field of aerospace engineering, particularly space crafts and rockets. As the results of this investigation reveal, vortex formation is suppressed at large values of D_2. To particularly note, at the highest value of D_2 (equals D_1), vortex air core formation is completely suppressed where maximum possible flow discharge is enabled through both the ports. In the case of liquid propellant storage tanks with single port draining which is the usual case of application, vortex formation prevents the outlet discharge of the propellant to the engine adversely affecting the launch capability (Agarwal *et al.*, 2014). As already discussed, introducing two drain ports instead of one (equivalent port) at identical conditions would suppress vortex formation to a significant extent of about 44%. In this context, it is suggested here that, if two drain ports are employed instead of one, besides suppressing the vortex air core, the propellant discharge flow rate could also be maintained unaffected thus keeping the space vehicle safe from the problems associated with residual propellants that could remain in the propellant tank otherwise. Hence, it is thought that, the present results provide a viable solution to the stability problems associated with space systems which are liable to be affected by air entraining vortices. On similar argument, the advantage of using twin drain ports in preventing vortexing could be extended to other areas such as hydraulic engineering (Padmanabhan, 1984) and metal casting (Sankaranarayanan and Guthrie, 2002).

The process of vortex air core formation is understood to be primarily due to axial flow-induced instability where, a sudden change over occurs from swirl flow to axial flow as a consequence of an initial dip formation at near the center (Chen and Winterthur, 1979). The resulting vortex air core is a Rankine vortex consisting of a forced vortex (central region) encircled by a free vortex swirl flow (Odgaard, 1986). It is also known that the boundary between the free and forced vortex regions (core edge) is unstable and is characterized by high turbulence (Chen and Winterthur, 1979; Binnie *et al.*, 1948). As the draining takes place, energy

transfer takes place from the potential vortex (outer flow regime) to the inner core increasing the angular velocity of the inner core (forced vortex) also reducing its radius (Chen and Winterthur, 1979). At some time instant during draining, due to the core edge instability, axial flow develops first in to a dip that further develops in to a full size vortex air core. That is, vortex air core formation is thought to be an instability phenomenon due to the feedback between the free and forced vortex regimes. Sohn *et al.* (2013) suggested that such an vortex air core formation is strongly linked to the intensity and spatial expansion of Torus-shaped Taylor vortex generated during the liquid draining process. However, it is surprising that, though there are two drain ports in the present study, there is only one vortex air core that is generated during draining. The characteristics of vortexing phenomenon during draining through two drain ports is plausibly be due to the mutual interaction between the flow fields around the drain ports bringing significant variations in the static pressures around them. This is particularly evident in a specific case of the present investigation where vortex suppression occurs when the drain ports carry equal diameters even at the highest initial rotation rate (n = 200 rpm) provided to the liquid column. Nonetheless, the precise reasons for the observed features, viz., variations in the critical height and liquid emptying time with fluid rotation speed are not known at present and more studies are required to bring out the physics involved.

4. CONCLUSIONS

Gas entrainment and resulting formation of Rankine vortex when a liquid is drained from a tank is a major adverse problem in many fields of engineering such as in flight of space vehicles, metal casting and hydraulic intakes. Hence, suppression of these vortices are warranted in such engineering applications. In contrast to all the previous studies where only single drain port is used, the current study investigates vortex air core (Rankine vortex) formation in a cylindrical vessel employing two drain ports to discharge the liquid (water) induced with a rotation. Unlike the case of single drain ports (previous studies), the current experimental results show that the vortex formation could be completely suppressed with liquid draining simultaneously enabled through two eccentric drain ports with equal size. In this study, the size of one of the drain ports is fixed (primary port) and the size of the other (secondary port) is varied. Eccentricity of the drain ports being varied, at smaller value of eccentricity, the critical submergence of vortex formation undergoes a continuous increase with fluid rotation speed but decreases as the size of the secondary port is increased. At larger eccentricity values, critical height registers an altogether different and non-linear course of variation characterized by an initial increase followed by a decrease with liquid rotation. In addition, smaller secondary port size gives rise to higher critical height which is quite contrary to the nature of vortex formation in case of liquid draining through single drain port. Visualization study bring to light an interesting feature of vortex air core, viz., it sways between the drain ports with a curvy surface profile apart from disclosing the nature of the drain port exit flow.

Previously reported results with single drain port reveal that the time of draining invariably increases when a rotated liquid column is drained compared to the case of simple draining (no rotation). But the present investigation reveals that for certain combination of fluid rotation speed, port size and port eccentricity, draining occurs more rapidly (that is, time of draining decreases) than in the case of liquid draining with no rotation. A mathematical treatise carried out as a part of the present study elucidates the efflux velocity change in fast draining case compared to the normal draining situation. Apart from illustrating the velocity contours, PIV results obtained show compliance to the possible changes the efflux (axial) velocity undergoes during the normal and fast draining cases studied. For fast draining case, the increase in the flow discharge (compared to the no rotation case) could be measured to physically confirm the result which is also visually reflected in the discharge outlet flow pattern obtained through flow visualization. One of the fascinating results of this study is the fact that, at identical conditions, twin port configuration allows faster draining compared to an equivalent single port by way of suppressing the vortex formation with higher discharge flow rate. This finding is thought to have tremendous application potential in space engineering (liquid propulsion systems) and hydraulic engineering where vortex suppression is much sought after to eliminate adverse effects. Additionally, the tangential velocity distribution obtained from PIV technique indicates that for normal draining case, there is Rankine vortex formation and for faster draining case, there is no full Rankine vortex formation. Furthermore, PIV results show that tangential velocity is considerably higher in normal draining case compared to that in the faster draining case at identical time instant.

ACKNOWLEDGMENTS

We are deeply grateful to Department of Mechanical Engineering, Amrita Vishwa Vidyapeetham (Deemed University), Amritapuri Campus, for granting us all the necessary apparatus and laboratory space, and further for all the motivation given to us to complete this work. Heartfelt thanks are also due to the CSIR-National Aerospace Laboratories, Bengaluru for enabling us to carry out the PIV experiments at its facility.

REFERENCES

Abramson, H., W. H. Chu, L. R. Garza and G. E. Ransleben (1962). *Some studies of liquid rotation and vortexing in rocket propellant tanks*. NASA technical note. National Aeronautics and Space Administration.

Agarwal, D., P. Basu, T. Tharakan and A. Salih (2014). Prediction of gas-core vortices during draining of liquid propellants from tanks.

Aerospace Science and Technology 32(1), 60-65.

AjithKumar, R., J. Joykutty, R. K. Shaji and A. R. Srikrishnan (2016). Vortex suppression through drain port sizing. *ASCE Journal of Aerospace Engineering* 29(4), 06016002.

AjithKumar, R., R. R. Nair, M. Prabhu and A. R. Srikrishnan (2017). Vortex formation during draining from cylindrical tanks: Effect of drain port eccentricity. *ASCE Journal of Aerospace Engineering* 30(5), 06017001.

Baum M. R. and M. E. Cook (1975). Gas entrainment at the free surface of a liquid: entrainment inception at a vortex with an unstable gas core. *Nuclear Engineering and Design* 32(2), 239-245.

Binnie, A. M., G. A. Hookings and G. I. Taylor (1948). Laboratory experiments on whirlpools. Proceedings of the Royal Society of London. Series A. *Mathematical and Physical Sciences* 194(1038), 398-415.

Chen, Y. N. (1979). From bathtub vortex to pump-intake vortex. *Schweizer Ingenieur und Architekt* 97, 845-852.

Fujimura, K., H. S. Koyama and J. M. Hyun (2004). An experimental study on vortex breakdown in a differentially rotating cylindrical container. *Experiments in Fluids* 36(3), 399-407.

Gluck, D. F., J. P. Gille, E. E. Zukoski and D. J. Simkin (1966). Distortion of a free surface during tank discharge. *Journal of Spacecraft and Rockets* 3(11), 1691–1692.

Gopikrishnan, T., U. Anandakrishnan, A. Sai Kiran, R. Ajith Kumar and T. Anith (2017). Vortexing during draining through twin drain ports in a cylindrical tank. *In 2017 2nd International Conference for Convergence in Technology (I2CT)*, 325–330. IEEE.

Gowda, B. H. L. (1996). Draining of liquids from tanks of square or rectangular cross sections. *Journal of Spacecraft and Rockets* 33(2), 311-312.

Gowda, B. H. L., P. J. Joshy and S. Swarnamani (1996). Device to suppress vortexing during draining from cylindrical tanks. *Journal of Spacecraft and Rockets* 33(4), 598–600.

Gowda, B. H. L., P. J. Joshy and S. Swarnamani (1997). Influence of vibration in the horizontal plane on discharge of discharge of liquid from a cylindrical tank. *Indian Journal of Engineering and Material Sciences* 4, 92–101.

Gowda, B. H. L., S. Akhuli, B. R. Anudeep, K. Ipe and K. Kishore (2013). Influence of base inclination on vortex formation during draining from cylindrical tanks. *Indian Journal of Engineering and Material Sciences* 20, 361–366.

Lubin, B. and G. Springer (1967). The formation of a dip on the surface of a liquid draining from a tank. *Journal of Fluid Mechanics* 29(2), 385-390.

Mizuki, S., B. H. L. Gowda and T. Uchibaba (2003). Visualization studies using PIV in a cylindrical tank with and without vortex suppressor. *Journal of Visualisation* 6(4), 337-342.

Mohammadi, J., H. Karimi, M. Islami and M. H. Hamedi (2012). The critical height of a liquid being drained from the tank with bell-mouth drain port. *Advances in Mechanical Engineering* 4, 1–5.

Odgaard, A. J. (1986). Free surface air core vortex. *Journal of Hydraulic Engineering* 112(7), 610-620.

Padmanabhan, M. (1984). Air ingestion due to free surface vortices. *Journal of Hydraulic Engineering* 110(12), 1855-1859.

Piva, M., M. Iglesias, P. Bissio and A. Calvo (2003). Experiments on vortex funnel formation during drainage. *Physica A: Statistical Mechanics and its Applications* 329(1), 1-6.

Ramamurthi, K. and J. Tharakan (1992). Shaped discharge ports for draining liquids. *Journal of Spacecraft and Rockets* 30(6), 786-788.

Sankaranarayanan, R. and R. I. L. Guthrie (2002). Slag entraining vortexing funnel formation during ladle teeming: similarity criteria and scale-up relationships. *Ironmaking & Steelmaking* 29(2), 147-153.

Sohn, C., B. Gowda and M. G. Ju (2008). Eccentric drain port to prevent vortexing during draining from cylindrical tanks. *Journal of Spacecraft and Rockets* 45(3), 638-640.

Sohn, C., J. H. Son and I. S. Park (2013). Numerical analysis of vortex core phenomenon during draining from cylinder tank for various initial swirling speeds and various tank and drain port sizes. *Journal of Hydrodynamics* 25(2), 183-195.

Takahashi, M., A. Inoue, M. Aritomi, Y. Takenaka and K. Suzuki (1988). Gas entrainment at free surface of liquid. *Journal of Nuclear Science and Technology* 25(3), 245-253.